

14th CIRP Conference on Intelligent Computation in Manufacturing Engineering, CIRP ICME '20

Automatised quality assessment in additive layer manufacturing using layer-by-layer surface measurements and deep learning

Léopold Le Roux^a, Chao Liu^a, Ze Ji^a, Pierre Kerfriden^{a,b}, Daniel Gage^c, Felix Feyer^c,
Carolyn Körner^c, Samuel Bigot^{a,*}

^aCardiff University, The Parade, Cardiff CF24 3AA, Wales

^bCentre des Matériaux, Mines ParisTech, Boulevard Saint-Michel, Paris 75 272, France

^cFriedrich-Alexander Universität, Erlangen-Nürnberg, Martensstraße 5, 91058 Erlangen, Germany

* Corresponding author. Tel.: +44 29208 75946. E-mail address: bigots@cardiff.ac.uk

Abstract

Additive manufacturing (AM) has gained high research interests in the past but comes with some drawbacks, such as the difficulty to do in-situ quality monitoring. In this paper, deep learning is used on electron-optical images taken during the Electron Beam Melting (EBM) process to classify the quality of AM layers to achieve automatized quality assessment. A comparative study of several mainstream Convolutional Neural Networks to classify the images has been conducted. The classification accuracy is up to 95 %, which demonstrates the great potential to support in-process layer quality control of EBM. And the error analysis has shown that some human misclassification were correctly classified by the Convolutional Neural Networks.

© 2021 The Authors. Published by Elsevier B.V.

This is an open access article under the CC BY-NC-ND license (<https://creativecommons.org/licenses/by-nc-nd/4.0>)

Peer-review under responsibility of the scientific committee of the 14th CIRP Conference on Intelligent Computation in Manufacturing Engineering, 15-17 July 2020.

Keywords: Artificial Intelligence; Additive Manufacturing; Quality control; Image recognition; Transfer learning

1. Introduction

Additive manufacturing (AM) is one of the fastest expanding manufacturing technologies in many industrial areas, making it a high-value research topic in a wide range of industrial applications. Creating nonstandard shaped parts can be a challenge with conventional manufacturing technologies, while the AM technologies' main strength is to enable the design and production of complicated shapes that could not be previously considered. However, the integration of AM technologies in the industry is still being limited due to various barriers. This is particularly true for Metal AM. For many industrial applications where production costs, geometrical tolerances and uniformities of material properties are critical, Metal AM remains a time-consuming and expensive process lacking repeatability in the quality of produced components.

This is due to the relative lack of maturity of Metal AM technologies. The quality and repeatability of AM processes is heavily dependent on the scientific understanding of the influence of printing parameters when processing specific materials. This has led to a wide range of scientific work to understand the influence of printing parameters [1] on the quality.

Despite this ongoing research work, many uncertainties regarding process parameters tuning remain in terms of achievable qualities, particularly when new materials/geometrical-features combinations are considered. This issue can also be difficult to tackle considering that with commercial Metal AM machines a limited number of AM parameters are available for user-led tuning, as manufacturers often protect control parameters specific to their personal expertise. Thus, in addition to the research activities on processing parameters mentioned above, many researchers

have been focusing on developing reliable monitoring systems analysing process signatures in an attempt to detect defects, as a first step, and if possible, to propose in-process corrections. Some examples of such attempts are the use of an acoustic emission to detect printing quality [2] or photodiode to assert the print quality [3].

In this paper, a new automatic quality classification method is presented and used to detect pores and bulging defects occurring when using an Electron Beam Melting (EBM) AM printer to process Ti-6Al-4V [4] powder. This classification method was developed using Artificial Intelligence (AI), and more specifically Convolutional Neural Network (CNN) models, to analyse EBM AM layers images collected during the printing with a wide variety of printing parameters to cover a wide range of printing conditions.

For this study, five of the most famous Deep Learning algorithms have been selected due to their popularity and good results, namely AlexNet, DenseNet, Resnet, SqueezeNet and VGG. Their performance, when applied to the detection of pores and bulging defects occurring in EBM AM, was then compared.

The remainder of this paper is organized as follows. Section 2 presents a literature review of relevant Metal AM and AI concepts. Section 3 introduces the selected EBM AM case study. Finally, section 4 discusses the experimental results and concludes the paper.

2. Literature review

2.1. Metal Additive manufacturing technologies

Various Metal AM technologies are emerging to produce metallic components and most of them create parts by stacking multiple layers of material on top of each other. Each technology has its own capabilities in terms of printing resolutions, processable materials and achievable geometries.

This paper will focus on Electron Beam Melting (EBM) technology, which melts metal powder using an electron beam [5]. This electron beam is created using a tungsten filament and an acceleration voltage of 60 kV (Fig. 1 a). This beam then goes through a group of lenses (Fig. 1 b) to focus and move the beam on the printing area (Fig. 1 c). Layers of raw powder are dispensed on the printing area using a rake (Fig. 1 d). The thickness of those layers is controlled by the users.

These parameters influence the required energy to correctly melt the layer, as a thicker layer need more energy from the electron beam but would lead to quicker printing. Not reaching the appropriate energy input can result in layers' defects in the form of porosity or deformations [4]. Thus, printing parameters tuning is an important research area as the tuning must be made for each type of powder. Research has been made by monitoring the powder bed to measure the impact of parameters variations [6]. Beam power, beam speed and volume energy density are the most common and used parameters to configure a print. More parameters exist, some can be hidden by the printer manufacturer as in Selective laser sintering (SLS), where at least 50 parameters influencing the print quality have been found [1].

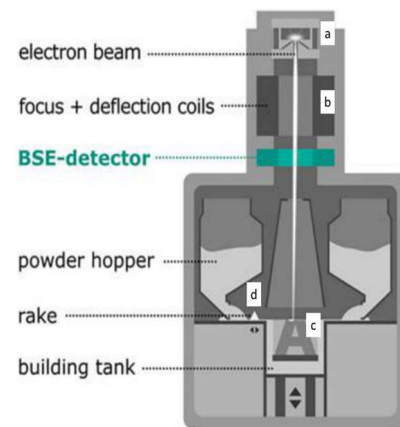


Fig. 1. Schematic of an EBM printer [5]

2.2. Machine learning

AI, specifically Machine Learning (ML), made a revolution in the way we classify and predict systems' future states by using historical data to create and train predictive models. The standard approaches used to train a learning model can be broadly classified in three different ways. One of the most widely adopted is supervised learning, which is used when the training dataset contains the desired output, known as labels, that must be predicted by ML models. For example, in images classification problems, training images generally need to be first classified by human experts to provide data to train the AI models. Those models will generalise this classification to be able to handle unseen images. When training datasets are not labelled or classified with a specific result or prediction, unsupervised learning can then be considered. This learning will then perform automatically a classification of new data by identifying clusters in the training data. And when dataset can be represented as an environment, reinforcement learning is used to explore and exploit this environment.

The type of learning and related algorithms are chosen in function of the type of datasets. Algorithms can also be tuned to work on a specific dataset by using transfer learning [7]. The transfer learning allows the use of algorithms pre-trained on similar datasets, which reduces the training time.

During the last decade, a technique called Deep Learning [8] [9] (DL) has gained popularity and is increasingly being used in various applications. One particular advantage of DL techniques is their ability to easily deal with the crucial task of features selection, which is essential to achieve accurate results. This makes DL techniques ideal candidates to develop intelligent monitoring systems for Metal AM, due to the expected complexity of the features representing defects in the monitored signals. In DL, different architectures can be implemented, each achieving better or worse results depending on the type of data. To classify images, for the type of data collected in the EBM AM case study presented in this paper, a CNN appears to be the most appropriate DL architecture [10]. As described below, CNN has made a revolution in the world of image recognition [9].

Thus, for the proposed case study, this paper is focusing on testing five well-known CNNs:

- AlexNet: AlexNet is the first CNN to win on 2012 ImageNet Large Scale Visual Recognition Challenge image recognition contest [11]. This achievement has allowed AlexNet to lead the way in the use of CNN in image recognition. Its architecture is composed of 8 layers: 5 convolutional layers for features extractions and 3 fully connected layers making the classification result.
- VGG: To obtain better performance than AlexNet, researchers have created a deeper neural network. This augmentation of the number of layers increases the capacity of the CNN to create an abstract representation of data but comes with some problems such as the vanishing gradient problem. VGG was created with a depth network of 19 layers and achieved top images recognition in images challenges [12].
- ResNet: ResNet CNN was made using skip connections to connect distance layers [13]. This avoids the vanishing gradients problem and makes it possible to create a deeper neural network.
- DenseNet: DenseNet is an evolution of ResNet. It is composed of multiple dense blocks separated by convolution and pooling layers [14]. Those dense blocks are made of multiple connected layers. Each layer is connected to all the following ones. DenseNet needs only 1/3 of ResNet parameters to obtain similar accuracies [14]. Making DenseNet more efficient.
- SqueezeNet: In 2016, SqueezeNet obtained equivalent results to AlexNet by using 50x fewer parameters [15]. This drastic parameters reduction was made by using convolution layers with smaller filters. This parameters reduction also allows a reduction in training time and produces lighter models.

2.3. Additive manufacturing with machine learning

In the literature, experiments have been made to monitor printing quality using ML and images extracted from the AM process. Scime and Beuth [16] focused on using data acquired by monitoring the melt pool to predict layers' quality. The printing quality was predicted by ML using filtered images. The acquisition of melt pool images requires the use of a high-speed camera to properly capture the physical phenomena. Thus, this experiment has generated 6 400 images per second (~13 GB per second), which are required to monitor the melt pool accurately, making real-time acquisition and analysis unrealistic.

In another study, Scime and Beuth [17] used powder bed images taken post melting for quality assessments. These techniques reduce the input data to a reasonable size for real-time control. However, this input size-reduction does not allow the control of the melt pool, which is at the origin of the majority of the defaults. Other studies [6] [18] used multiple images of one layer to make quality assessments. Those images give a different type of information on the print. This study uses layer images before and after scanning, to look at defects in the powder affecting the printing and the parts' quality.

Our study will use a different type of images to detect in-process defects, namely electron-optical (ELO) images, as they can help visualize topography surface changes [5].

3. AM case study, a quality classification of EBM layers

3.1. EBM printing process summary

To use the EBM process, first, a CAD model is created and the printing orientation is selected. This orientation will influence how the final product will be and how a defect will affect the final result. This CAD model is then sliced in multiple layers and converted in machine code. This conversion requires printing parameters, such as the layer thickness, the scanning patterns (defining the scanning path) and the scanning speed.

During printing, deviations may occur as the defined printing parameters may not be fully respected or may be influenced by unexpected deviations, such as temperatures or powder bed quality variations. Those variations can be monitored by monitoring various process signatures, such as layer images or sound as shown in Figure 2 [2]. Various types of layers images can be used to detect porosity, bulging, temperature variations or layer deposition problems. Sounds may allow detection of issues with the powder recoater, such as impacts with the produced parts due to geometrical deformations. Other sensors can also be used, such as thermal sensors to monitor the stability of the melt pool. After printing, the part itself can be checked to provide more feedback on the process. Internal and external features can be measured (e.g. porosity, microstructure, dimensional accuracy) using various metrology tools (e.g. microscope, CT scans).

This paper focuses on the capture of ELO images obtained by detecting backscattered electrons (BSE) [4]. Those sensors are located on the top of the building chamber allowing monitoring of the real state of each layer. The assumption being that the use of layer images, rather than monitoring the melt pool, would still provide sufficient information to detect deviations, while allowing a data size small enough to implement real-time analyses and potentially real-time correction in the next layer.

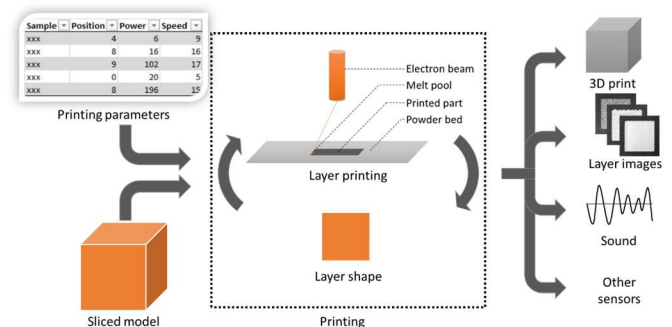


Fig. 2. Input and output of a 3D printing

3.2. Experimental setup and collected images

Simple 15 mm by 15 mm cubical parts were produced by EBM using various scanning speeds and beam powers [4] [5], leading to 2 types of defects, namely porosity and bulging. Throughout the AM process 16,324 ELO images of the printed layers were collected.

These images were then classified by a human expert in one of the 3 defined categories: porous, normal or bulging. As classification is a monotonous task, human errors are expected and some layers can have features of multiple classes, making them hard to classify.

The porous category (Figure 3.a) is due to too low energy input caused by an insufficient beam power or an excessive beam speed resulting in the creation of pores in the layers. Those pores can be easily identified by a human as their characteristics are well known. They have the appearance of a black dot in the printing area.

The second category, the bulging category (Figure 3.b), is the opposite of the first one. The excess of energy during the printing makes the printed layer wrap and deform. It can be caused by having low beam speed or high beam power.

In some cases, bulging over several layers can lead to pores resulting in a porous and bulging layer as seen in Figure 3d. This case can make data analysts, who lack the domain knowledge, fail to recognize the layer category. This type of layer was the hardest to classify.

The third category is the good quality print where none of the previous defaults exists as in Figure 3c.

The image data set included 6954 porous images (43 %); 3167 bulging images (19 %), and 6203 normal images (38 %).

3.3. Data pre-processing

Data pre-processing consisted of extracting the print part from the powder bed (Figure 4), as the powder bed does not contain any information. The edge of the print was also removed to protect against border artefacts, which may create confusion in the CNN training. Next, images were normalized using hard-coded values to avoid learning from unrelated features.

Removing the corner of the printed part should make it possible to use the produced neural network for the analyses of

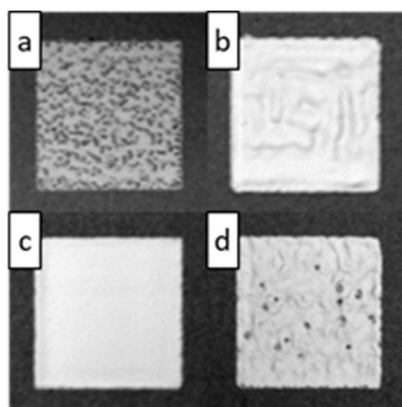


Fig. 3. ELO images of layers types

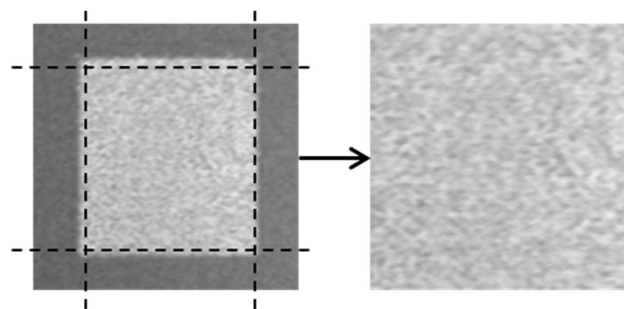


Fig. 4. Images pre-processing

different printed shapes as it will only classify the inner part of the print without using the print border.

3.4. Data processing with CNN

For this research, Python 3.7.4 and Pytorch 1.3.1 were used. Calculations were performed on the supercomputer ARCCA using P100 GPU. The uses of graphics cards speed up the data processing time, making possible to classify on images in less than 0.01s. The CNNs presented in section 2.2 were used as a straight forward solution to classify the images using Pytorch [19]. The CNNs training was done using the same hyperparameters for all. Their momentum was set to 0.9 and the learning rate to 0.001.

To process those images, each CNN was trained twice, once with transfer learning (called pre-trained) and once without it (called untrained). This allows to compare the capacity of the CNNs to learn from scratch on the data. With transfer learning, a previous CNN had been trained on complex datasets and had learned to extract features from images. Thus, transfer learning copies the weights of this existing CNN in the new CNN, consequently transferring some of its feature extraction capabilities.

The comparison test shows, as expected, that pre-trained CNNs have overall better accuracy and faster training than untrained CNNs. But untrained CNN's models demonstrate more significant differences in performance.

Training results are shown in Figure 5 and Figure 6. The top accuracy was obtained with a pre-trained SqueezeNet (95.1 %). But surprisingly, AlexNet without pre-training did not learn effectively. Its accuracy stabilises itself around 33 % looking like a random choice (as shown in Figure 6). As the pre-trained

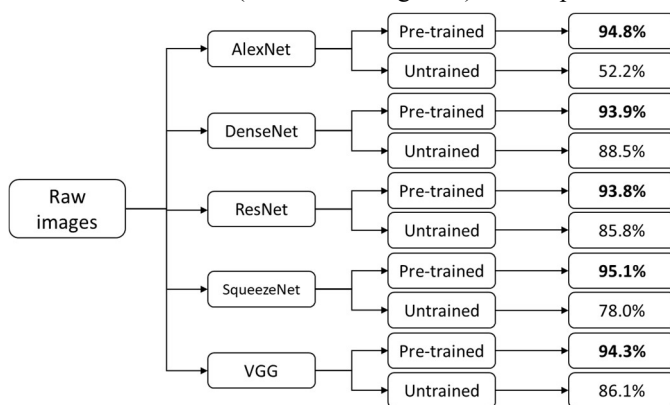


Fig. 5. Top accuracy comparison

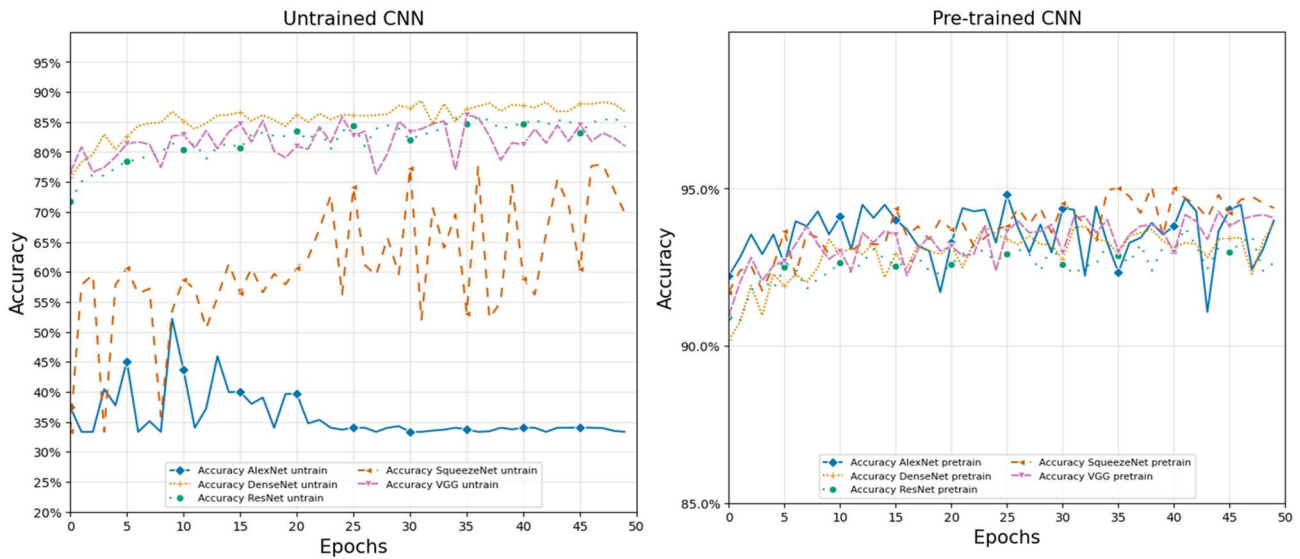


Fig. 6. CNNs accuracy curves

CNNs produced better results, the focus will be on them. It was found that their accuracies will quickly approach 95% and then stop improving thereafter. As shown in Figure 6, the learning of the CNN quickly stops as the accuracy starts to stabilise near the 10th epoch.

The accuracy showed for each algorithm is the validation accuracy. Obtained by checking the model prediction on new data, unseen during the training. The advantage of focusing on the validation accuracy rather than on the training accuracy is that it can highlight any overfitting, where the neural network learns irrelevant features and can't generalise properly on new data. The training data and the validation data used were the same for all models.

3.5. Errors analysis

The CNN accuracy appears to be topped around 95 %, suggesting that the 5 % of inaccuracy could be caused by noises in the data that may be due to human errors, during the classification by an expert, or due to ambiguities to categorize images. To investigate this further, a confusion matrix of a pre-trained SqueezeNet CNN was constructed (Figure 7). 0 represents the layers classified as normal, 1 the ones classified as porous and 2 the ones classified as bulging.

By highlighting how the CNN classifies the images in comparison with the human expert classification, the confusion

matrix should help detect which type of images are creating confusion.

To construct the matrix (Figure 7), 20 % of the available images were used. They were selected randomly, while providing the same amount of each image type, and submitted for prediction to a trained SqueezeNet CNN. Then, for each expected image type, as classified according to the human expert, the percentage of image predicted as belonging to each of the three types was calculated and added to the confusion matrix (Figure 7).

Focusing on the highest classification mismatches, the confusion matrix shows that the CNN is classifying 3 % (cell [0,2]) of the images as bulging while, according to the human expert, they should be classified as normal, while classifying 0.8 % (cell [2,0]) as normal while they should be classified as bulging, leading to a total classification error of 5 %. This suggests that distinctions between the normal and bulging images bring some difficulties to either the CNN or the human expert. By examining the images more closely, this confusion could be explained. To help visualise the problem, 9 classified images have been extracted and placed in the confusion matrix (Figure 8).

This figure shows some images, in particular cells [0,2] and [2,0], which result in mismatches due to slightly visible bulging. Slight bulging is tolerable and therefore categorized as normal by the human expert, but a quantitative and sharp

		Human Classification		
		Normal 0	Porous 1	Bulging 2
CNN Classification	Normal 0	30 %	1.3 %	0.8 %
	Porous 1	0.54 %	32 %	0.13 %
	Bulging 2	3 %	0.31 %	32 %

Fig. 7. Confusion matrix of pre-trained Squeezenet

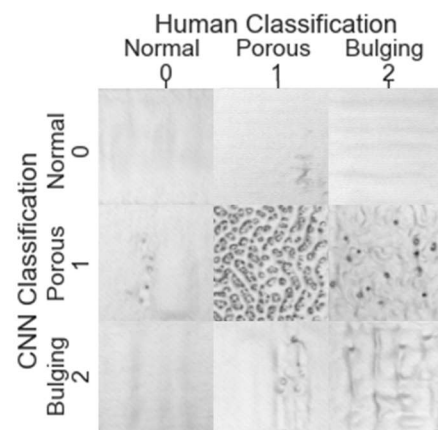


Fig. 8. Confusion matrix with images

transition between non-tolerable bulging and layers categorized as normal is still missing.

With that in mind, the monotonous task of classifying such images is likely to bring human errors and while such errors could have been present during the CNN training. Thus, rather than a wrong classification by the CNN, these classification mismatches are more likely to highlight a human error. Therefore, the CNN performance is likely to be higher than the plateau mentioned previously.

The last two highest mismatches are shown in cells [1,0] and [1,2], where images classified as porous by the human expert, were predicted as normal (1.3 %) or as bulging (0.31 %) by the CNN. Looking at some of the related images (Figure 8), they appear to contain features from both defects and may suggest that such images would be hard to classify by both a CNN and a human expert. To solve this problem, an additional class for layers with both defect types, pores and bulging, have to be complemented.

4. Conclusion and future work

The results showed that ELO images can be correctly classified by a CNN without too much difficulty allowing automatic monitoring of the state of printing in real-time, as the time required to classify one image is inferior to 0.01 s on a graphic card, which is much shorter than the time needed to print a layer. An un-trained CNN had more difficulties to learn from the data set and did not achieve the good accuracies that a pre-trained CNN did. This can be due to the similarity between all images, which may confuse the network and making it overfit the data by learning non-relevant patterns. While pre-train neural networks have been first trained on more diverse data, forcing them to extract good features.

This work proves that the EBM printing quality of a single layer can be monitored in real-time using ELO images with great accuracy (95%) leading to the development of ML feedback loops [20]. But these detected defects could still be modified by the processing of future layers, mainly because of multiple remelting. For example, detected pores could vanish by sufficient energy input in the subsequent layers. Those changes can lead to uncertainty in the layers' defect classification and especially in the correlation of layer defects and defects in printed parts. Future work will focus on collecting data after a completed build, for example using CT-scans, to link information brought by ELO images during the process of a layer with the actual resulting layer inside a completed part.

Acknowledgements

This work was performed using the computational facilities of the Advanced Research Computing @ Cardiff (ARCCA) Division, Cardiff University.

This project has received funding from the European Union's Horizon 2020 research and innovation programme under grant agreement n°820774.

References

- [1] Amimi, M., and Chang, S. Process Monitoring of 3D Metal Printing in Industrial Scale. ASME 2018 13th Int. Manuf. Sci. Eng. Conf. MSEC 2018.
- [2] Shevchik, S. A., Kenel, C., Leinenbach, C., and Wasmer, K. Acoustic Emission for in Situ Quality Monitoring in Additive Manufacturing Using Spectral Convolutional Neural Networks. *Addit. Manuf.*; 2018. p. 598–604.
- [3] Okaro, I. A., Jayasinghe, S., Sutcliffe, C., Black, K., Paoletti, P., and Green, P. L. Automatic Fault Detection for Laser Powder-Bed Fusion Using Semi-Supervised Machine Learning. *Addit. Manuf.*; 2019. p. 42–53.
- [4] Pobel, C. R., Arnold, C., Osmanlic, F., Fu, Z., and Körner C. Immediate Development of Processing Windows for Selective Electron Beam Melting Using Layerwise Monitoring via Backscattered Electron Detection. *Mater. Lett.*; 2019. p. 70–72.
- [5] Arnold, C., Pobel, C., Osmanlic, F., and Körner, C. Layerwise Monitoring of Electron Beam Melting via Backscatter Electron Detection. *Rapid Prototyp.*; 2018. p. 1401–1406.
- [6] Imani, F., Gaikwad, A., Montazeri, M., Rao, P., Yang, H., and Reutzel, E. Layerwise In-Process Quality Monitoring in Laser Powder Bed Fusion. ASME 2018 13th Int. Manuf. Sci. Eng. Conf. MSEC 2018.
- [7] Weiss, K., Khoshgoftaar, T. M., and Wang, D. D. A Survey of Transfer Learning, Springer International Publishing; 2016.
- [8] Al-Saffar, A. A. M., Tao, H., and Talab, M. A. Review of Deep Convolution Neural Network in Image Classification. *Proceeding - 2017 Int. Conf. Radar, Antenna, Microwave, Electron. Telecommun. ICRAMET 2017*; p. 26–31.
- [9] Lecun, Y., Bengio, Y., and Hinton, G., Deep Learning. *Nature*; 2015. p. 436–444.
- [10] Guo, Y., Liu, Y., Oerlemans, A., Lao, S., Wu, S., and Lew, M. S. Deep Learning for Visual Understanding: A Review. *Neurocomputing*; 2016. p. 27–48.
- [11] Krizhevsky A, S. I., and G, H. ImageNet Classification with Deep Convolutional Neural Networks; 2017. *Commun. ACM*.
- [12] Simonyan, K., and Zisserman, A. Very Deep Convolutional Networks for Large-Scale Image Recognition. *3rd Int. Conf. Learn. Represent. ICLR 2015*; 2015. p. 1–14.
- [13] He, K., Zhang, X., Ren, S., and Sun, J. Deep Residual Learning for Image Recognition. *Proc. IEEE Comput. Soc. Conf. Comput. Vis. Pattern Recognit.*; 2016. p. 770–778.
- [14] Huang, G., Liu, Z., Van Der Maaten, L., and Weinberger, K. Q. Densely Connected Convolutional Networks. *Proc. - 30th IEEE Conf. Comput. Vis. Pattern Recognition, CVPR 2017*; p. 2261–2269.
- [15] Iandola, F. N., Han, S., Moskewicz, M. W., Ashraf, K., Dally, W. J., and Keutzer, K. SqueezeNet: AlexNet-Level Accuracy with 50 X FEWER PARAMETERS AND < 0.5 MB MODEL SIZE. *ICLR*; 2017. p. 1–13.
- [16] Scime, L., and Beuth, J., Using Machine Learning to Identify In-Situ Melt Pool Signatures Indicative of Flaw Formation in a Laser Powder Bed Fusion Additive Manufacturing Process. *Addit. Manuf.*; 2019. p. 151–165.
- [17] Scime, L., and Beuth, J. A Multi-Scale Convolutional Neural Network for Autonomous Anomaly Detection and Classification in a Laser Powder Bed Fusion Additive Manufacturing Process. *Addit. Manuf.*; 2018. p. 273–286.
- [18] Caggiano, A., Zhang, J., Alfieri, V., Caiazzo, F., Gao, R., and Teti, R. Machine Learning-Based Image Processing for on-Line Defect Recognition in Additive Manufacturing. *CIRP Ann.* 2019. p. 451–454.
- [19] Paszke, A., Gross, S., Massa, F., Lerer, A., Bradbury, J., Chanan, G., Killeen, T., Lin, Z., Gimelshein, N., Antiga, L., Desmaison, A., Köpf, A., Yang, E., DeVito, Z., Raison, M., Tejani, A., Chilamkurthy, S., Steiner, B., Fang, L., Bai, J., and Chintala, S. PyTorch: An Imperative Style, High-Performance Deep Learning Library. *NeurIPS*; 2019.
- [20] C., Liu, L., Le Roux, Z., Ji, P., Kerfriden, F., Lacan, S., Bigot. Machine Learning-Enabled Feedback Loops for Metal Powder Bed Fusion Additive Manufacturing. *Journal of Manufacturing Systems*; 2020.